

Computational Probes into the Basis of Silver Ion Chromatography. II. Silver(I)–Olefin Complexes

Jose Kaneti,^{†,‡} Louis C. P. M. de Smet,[†] Remko Boom,[§] Han Zuilhof,^{*,†} and Ernst J. R. Sudhölter^{*,†}

Laboratory of Organic Chemistry and Food and Bioprocess Engineering, Wageningen University, Dreijenplein 8, 6703 HB Wageningen, The Netherlands, and Institute of Organic Chemistry, Bulgarian Academy of Sciences, Acad. G. Bonchev str., Block 9, 1113 Sofia, Bulgaria

Received: April 17, 2002; In Final Form: August 27, 2002

Alkene complexes of silver(I) are studied by four computational methodologies: ab initio RHF, MP2, and MP4 computations, and density functional B3LYP computations, with a variety of all-electron and effective core potential basis sets. Methodological studies indicate that MP2/SBK(d) computations can adequately represent Ag(I)–alkene complexes, and this method is used to study Ag(I) complexes with one to six ethene ligands as well as with methyl-substituted ethene derivatives. The first two alkene ligands enter the coordination sphere of Ag(I) with approximately the same energy, in line with ICR experiments. The association enthalpies of additional complexing ethene ligands diminish progressively. Computations on methyl-substituted alkenes show that the observed trends in argentation chromatography are opposite to those observed and computed for the gas phase, and suggest strong medium effects in Ag(I) chromatography.

Introduction

The interactions between cations and π -electron systems currently attract significant attention, both by experimental and by theoretical investigations. Such interactions have important biological implications, as shown, e.g., by Dougherty and others on the interaction of cations with aromatic π -systems.¹ For nonaromatic π -systems, the archetypal metal– π bond is formed by the ‘two-electron–three-center’ bonding between silver(I) cations and alkenes.² This type of chemical bonding offers significant practical possibilities, as exemplified in high-performance liquid chromatography (HPLC) of terpenes.³ Since such materials play a crucial role in many biological processes, their purification (in optically active form) is of significant interest. Therefore, detailed knowledge of the types of interactions between Ag(I) and (functionalized) alkenes that play a role in such separations is highly desirable.

Metal–olefin binding interactions have been the focus of a number of theoretical studies over the last years.⁴ This three-center bonding is usually attributed to three different factors: electrostatic (ion–dipole) interactions, electron donation from occupied alkene π -orbitals to empty s-orbitals of the transition metal, and back-donation from filled metal d-orbitals to the unoccupied π^* -orbital of the alkene or alkyne (Figure 1).⁵ The relative contribution of these three factors in metal–alkene complexes forms the topic of an ongoing dispute. Not less than five methods have been applied to analyze the bonding situation in these complexes:^{4,6} natural bond orbital analysis (NBO),⁷ charge distribution analysis (CDA),⁸ atoms-in-molecules (AIM) method,⁹ energy decomposition analysis (EDA),^{10,11} and reduced variational space, RVS,¹² sometimes also referred to as con-

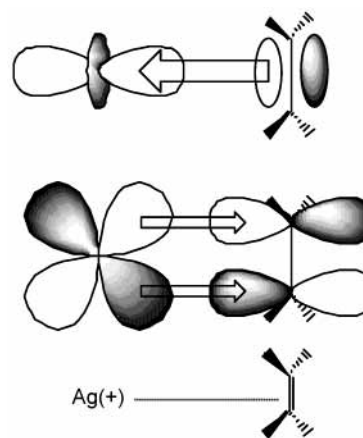


Figure 1. Silver(I)–alkene bonding: π – s^* donation (top) and d – π^* back-donation (middle) interactions as relevant for the Ag^+ – $(\text{C}_2\text{H}_4)_n$ complexes under study ($n = 1$ –4, 6).

strained space orbital variation (CSOV). On the basis of such analyses, three very different positions relating to the bonding situation have recently been defended: (1) By and large, the bonding is caused by electrostatic effects; electronic effects (π – s^* bonding and d – π^* back-bonding) are both small in comparison.¹³ (2) Ligand $\pi \rightarrow$ metal s^* electron donation and electrostatics dominate, while d – π^* back-bonding plays only a small role.^{4,15} (3) All three factors contribute to a significant degree to the complexation,¹⁴ and it has even been stated that the involvement of d-orbitals makes it “unreasonable to consider” such complexes as being dominated by noncovalent interactions.¹

Several theoretical studies reproduce correctly the complexation energy of Ag(I) with ethene by accounting for electron correlation up to the CCSD(T) level with large basis set reference wave functions,¹⁵ or via stepwise methodological approximations.¹⁶ However, we need a theoretical approach fast

* Address correspondence to either of these authors. E-mail H.Z.: Han.Zuilhof@phys.oc.wau.nl; e-mail E.J.R.S.: Ernst.Sudhölter@phys.oc.wau.nl.

[†] Laboratory of Organic Chemistry, Wageningen University.

[‡] Institute of Organic Chemistry, Bulgarian Academy of Sciences.

[§] Food and Bioprocess Engineering, Wageningen University.

enough to be applicable to larger complexes of interest, which is the methodological aim of this study, and accurate enough to properly represent the type of Ag(I)–alkene bonding revealed by studies using large all-electron or effective potential basis sets with extensive account for electron correlation.¹⁵ This study also aims at more insight in the reasons behind the disparity in opinions about the nature of the Ag(I)–alkene bond. Subsequently, we concentrate on finding the coordination number of Ag(I) for the terpene complexes of interest by studying the complexation of an increasing number of alkene ligands.

This theoretical analysis includes a study of the relevance of relativistic effects. The influence of relativistic effects in analytical or organic chemistry is usually negligible, and dismissed as belonging to the realm of ‘hard-core physics’ only. The situation in complexes of heavier transition metals can be qualitatively different.¹⁷ Due to the large positive charge of the nucleus, the electrons in especially the 1s-orbitals obtain very large kinetic energies. As a result, the effective mass of the 1s electrons in Ag is ca. 1.08 times the rest mass of the electron. Hence, the 1s-orbitals contract, which results in increased shielding. Other core orbitals (specifically s-type) will also contract, while in contrast, d- and f-type orbitals will expand in space, and go up in energy.¹⁸ The relevance of this effect has recently been shown in a comparative study of the complexation of Cu(I),¹⁵ Ag(I), and Au(I) to ethene.^{15,19} Although the relativistic effect increases in the sequence Ag(I) < Cu(I) < Au(I), the relativistic contribution to the bonding of Ag(I) and ethene has still been computed to amount to no less than ca. 10 kcal/mol using the EDA approach.¹⁵

In this paper, we report an in-depth study of three classes of compounds: (a) the cationic Ag(I)–ethene complex by a variety of methods, to find out which methods are accurate and fast enough to allow for the application to larger complexes; (b) complexes of Ag(I) with multiple ethene molecules, to obtain insight in the possible binding modes of molecules with multiple alkene complexation sites, such as in terpenes; (c) Complexes of Ag(I) with methyl-substituted ethene derivatives, to study the influence of alkyl substitution.

Methodological Details

Model complexes of Ag(I) are studied by ab initio MO and by density functional B3LYP²⁰ calculations with several effective core potential (ECP) basis sets: Hay-Wadt (HW),²¹ Stevens-Basch-Krauss (SBK)²² (denoted CEP-31G in Gaussian98²³) with polarization functions on non-hydrogen atoms, LANL2DZ,²⁴ and SDD.²⁵ Geometry optimizations with the latter two basis sets have been carried out using the Gaussian98 suite of programs,²³ which has been used also for the NBO analyses.⁷ The SBK(d) alias CEP-31G(d) basis set has been used along with MP2²⁶ geometry optimizations, mostly under the parallel version of GAMESS,²⁷ and with MP4 single point computations. There is a difference in the treatment of the polarization functions in the SBK(d) basis set in GAMESS, and the CEP-31G(d) basis set in Gaussian98: Gaussian98 adds a d-polarization function on Ag with the exponent 0.175, which GAMESS(US) does not do. In addition, the second and third row d-polarization functions in Gaussian98 have the exponent 0.75, while GAMESS uses as standard exponents for d-polarization functions on the same atoms 0.8. While the differences in second and third row polarization exponents have a negligible effect on calculated relative energies, the d-polarization function on Ag influences the calculated absolute and relative energies of Ag(I)–alkene complexes more significantly. Therefore, to make the results from the two program systems compatible, a d-polarization

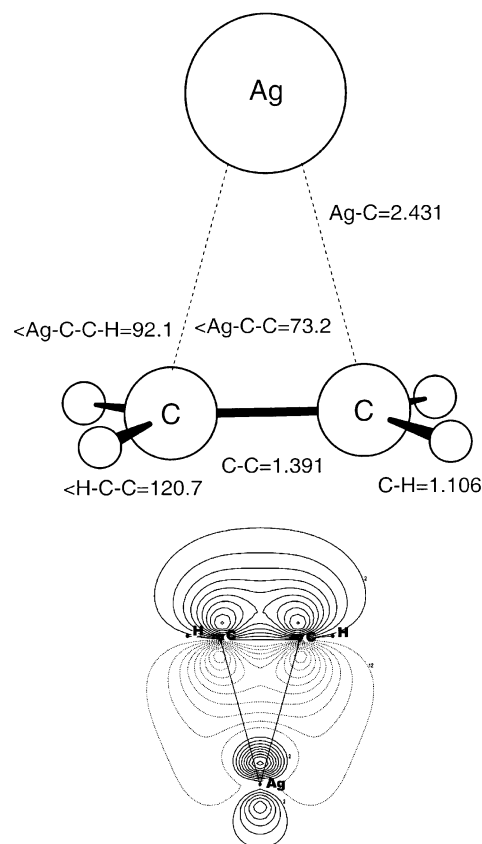


Figure 2. MP2/SBK(d) optimized geometry of the Ag(I)–C₂H₄ complex, with selected geometrical features (top), and the corresponding HOMO isodensity map (bottom). On the latter, the notations 2 and 12 respectively correspond to positive and negative density contours of 0.125 e.

function with exponent 0.175 has been added to the Ag basis set also in GAMESS–US calculations.

All MP2 computations use the frozen core approximation, and the MP4 computations are of the MP4(SDQ type). Relativistic effects on the bonding energy of studied complexes have been calculated explicitly using the scheme for Relativistic Elimination of Small Components (RESC)¹⁹ of the full four-component Dirac equation, implemented as a perturbation to the various Hamiltonian operators in GAMESS.²⁷ Alternatively, relativistic corrections are included statically via the effective potentials of LANL2DZ in Gaussian98.²³

Basis set superposition errors are—wherever required—accounted for by the counterpoise method (CP).²⁸ Graphics of computed theoretical structures, orbital and electron density maps, are rendered using the MOLDEN²⁹ and Chem3D³⁰ programs.

Results and Discussion

A. Geometry of the Ag(I)–Ethene Complex. The complex of Ag(I) and ethene as computed by the different methods used in this study has the characteristic T-shape with C_{2v} symmetry that has also been found in previous work.^{4,15} A typical result is presented in Figure 2 (top), and displays the MP2/SBK(d) optimized geometry of this complex. The corresponding orbital picture is illustrated using the HOMO isodensity plot of the Ag(I)–C₂H₄ complex (Figure 2, bottom). Two interactions are clearly visible here. First, only a small positive orbital overlap is visible between a (horizontally oriented) d-orbital of Ag and the π -orbitals of the ethene ligand. Second, another d-orbital lobe of Ag⁺ is directed toward the ethene π -orbital, but has an

TABLE 1: Selected Theoretical Geometry Parameters of the Ag(I)–C₂H₄ Complex

method/basis set	$R_{\text{Ag}-\text{C}}$ (Å)	$\Delta R_{\text{C}-\text{C}}^a$ (Å)	$\angle\text{HCCH}^b$ (deg)
HF/LANL2DZ	2.444	0.035	171.0
HF/SBK(d)	2.570	0.034	172.9
(HF + RESC)/SBK(d)	2.570	0.034	172.9
MP2/LANL2DZ	2.550	0.054	170.0
MP2/SBK(d)	2.429	0.064	170.8
(MP2 + RESC)/SBK(d)	2.429	0.065	170.8
B3LYP/LANL2DZ ^c	2.444	0.035	171.0
B3LYP/LANL2DZ	2.450	0.055	169.6
B3LYP/SBK(d)	2.389	0.064	169.7

^a Difference from the experimental gas-phase value for ethylene.

^b The 'trans'-dihedral angle. ^c Basis set: LANL2DZ for Ag; 6-311G(d,p) for C, H.

opposite sign, and is therefore responsible for a significant repulsive part of the Ag(I)–ethene interaction. Therefore, there seems to be only little covalent interaction between the metal and the ligand due to the simultaneous involvement of multiple d-orbitals.

Although the symmetry is method-independent, the precise calculated geometries vary somewhat from method to method. Only slight variations (≤ 0.03 Å) are found for the C=C distance, but the Ag–C distance was found to vary over ca. 0.2 Å from 2.39 Å (B3LYP/SBK(d)) to 2.57 Å (HF/SBK(d)) (see Table 1). The variations are largely due to differences in the treatment of electron correlation (e.g., HF versus MP2 and B3LYP), but are also influenced by basis set effects. Literature MP2 results, combined with our data, indicate a significant basis set dependence of the predicted geometry of Ag(I) complexes: ¹⁵ a stepwise increase of the basis sets on Ag and C by addition of polarization functions systematically shortens the Ag–C bond length. In this, selective addition of d-polarization functions on carbon has a somewhat larger effect than addition of analogous 5d-polarization functions on silver (see Table 1), as expected for the interaction between a cation and a neutral, polarizable ligand. Since no experimental geometry of the Ag(I)–C₂H₄ complex is presently known, it is of relevance to point out that concerning the energy of the complex only relatively small effects of the basis set size (beyond a minimum size) can be noted, and that in this comparison the largest basis sets at the MP2 level do not give the most accurate results (vide infra). This provides an additional reason (next to the necessity to use a constant, well-balanced basis set) to apply systematically the SBK(d) basis set to all atoms of the studied Ag(I) complexes.

The comparison of our DFT calculations (Table 1) with earlier results shows that B3LYP with the [10s/8p/7d/1f]/(9s/5p/6d/1f) basis set for Ag and a TZ2P basis set for C gives a Ag–C distance of 2.373 Å,¹⁵ close to our B3LYP/SBK(d) value of 2.389 Å. These results display the rapid convergence of the DFT geometry predictions upon increase of the basis set to a value of ca. 2.38 Å for the Ag–C distance.³¹ However, as long as no experimental data are available for the geometry of Ag(I)–C₂H₄, it is still unknown whether the DFT results are correct in this regard. Therefore, other criteria should be used to determine the quality of the methods at hand (see section B below).

The larger dependence of the Ag–C distance on the addition of d-polarization functions on C than on addition of 5d-polarization functions on Ag seems to indicate dominating ethene ligand donation, with less significant Ag(I) back-donation. Thus, the result favors the less covalent and largely electrostatic model of Ag(I)–ethene interactions of Bauschlicher et al.^{13c} or Frenking et al.,³² rather than the more covalent model obtained via large basis DFT and CCSD(T) calculations.¹⁵

TABLE 2: Binding Enthalpy of the Ag(I)–C₂H₄ Complex

method/basis set	ΔE (kcal·mol ⁻¹)
HF/LANL2DZ	-20.0
HF/SBK(d)	-24.0
(HF+RESC)/SBK(d)	-24.4
MP2/LANL2DZ	-26.4
MP4/LANL2DZ//MP2/LANL2DZ	-25.3
MP2/SBK(d)	-33.7
(MP2+RESC)/SBK(d)	-34.1
MP4(SDQ)/SBK(d)//MP2/SBK(d)	-32.5
B3LYP/LANL2DZ ^{a,b}	-33.5
B3LYP/SBK(d) ^a	-41.4
CCSD(T)/10s8p7d1f (ref 6)	-32.9
experimental (ICR) (ref Y)	-33.7

^a Corrected for basis set superposition errors. ^b LANL2DZ basis for Ag; 6-311G(d,p) for C, H, O.

This would be in line with the observation that the excitation of 3d → 4s in Cu(I) requires ca. 3 eV (75 kcal·mol⁻¹), while the 4d → 5s excitation in Ag(I) requires almost 6 eV (131 kcal·mol⁻¹).^{39,40,33} These excitation energies underscore decisively the considerably smaller capacity of Ag(I) to d–π* back-donation than of Cu(I), and, therefore, point again toward the much less covalent character of the Ag(I)–C(π) interaction in comparison with the Cu(I)–C(π) interaction. The more general relevance of this is exemplified by the observation that even topological analyses of bonding⁹ between group XI metal cations and ethene supply controversial, basis set-dependent results⁴ as to whether the M(I)–C₂H₄ bonding is mostly covalent¹⁵ (i.e., showing a ring critical point) or mostly electrostatic³² (i.e., showing a critical point coinciding with the midpoint of the C=C bond, thus indicating an elongated T-shaped structure of the complex, which is the case for Ag(I)–C₂H₄).

Another possible reason for the difference in calculated Ag(I)–C distances of present MP2/SBK(d) calculations and earlier MP2 and CCSD(T) results¹⁵ might be the influence of relativistic effects on the electrons of silver. Therefore, we have also investigated relativistic effects explicitly within the recently introduced RESC scheme,^{19,27} related to the known decoupling of large and small spin–orbital elements of the Dirac equation.³⁴ Incorporation of relativistic effects in both HF/SBK(d) and MP2/SBK(d) geometry optimizations shows only marginal changes of geometry compared to the nonrelativistic HF and MP2 computations: all bond lengths changes are ≤ 0.001 Å. This is a strong indication of negligible relativistic effects on the geometries of Ag(I)–alkene complexes.

B. Energetics of Ag(I)–Ethene Complexes. Relatively little experimental data on dissociation energies of Ag(I) complexes with alkenes have been reported. To add to the complexity of the comparison between computed and experimental data, some experimental data are gas-phase stabilization energies,³⁵ while others are solid-phase heats of adsorption.³⁶ In Table 2 we compare the computed interaction energy obtained by several different theoretical approaches with the experimentally obtained interaction energy.³⁵ For the B3LYP computation, the basis set superposition error is accounted for by the counterpoise method. With the LANL2DZ basis for Ag and 6-311G(d,p) for C and H, the computed counterpoise BSSE, B3LYP, is 0.8 kcal·mol⁻¹, confirming the earlier conclusions of small BSSEs in DFT calculations.¹⁵ The BSSE for MP2 is expected to be negligible due to internal cancellation.^{15,37} In Table 2, both the experimental value and the computational CCSD(T)/10s8p7d1f value (presently the highest computational level at which this complex has been studied) are added as references.

Our MP2/SBK(d) computations give excellent reproduction, within experimental error, of the experimental complexation

energy. Further increase of the basis set, to obtain MP2/10s8p7d1f results, yields an overestimation of $3 \text{ kcal}\cdot\text{mol}^{-1}$,¹⁵ supporting our choice of the SBK(d) basis set. No clear trend in the basis set dependence is apparent from the B3LYP-computed Ag(I)–ethene interaction energies. The moderate size LANL2DZ basis set reproduces the experimental dissociation energy of Ag(I)–C₂H₄ (Table 2). However, B3LYP computations with the larger (10s8p7d1f)¹⁵ and CEP-31G(d) basis sets overestimate the Ag(I)–C₂H₄ dissociation energy by 3 and 8 kcal/mol, respectively.

Apart from the basis set, the theoretical method used also influences the interaction energies. MP2 computations with a large enough basis set (SBK(d) rather than LANL2DZ) provide a good agreement with experiment. Single point MP4(SDQ)/LANL2DZ and MP4(SDQ)/SBK(d) calculations yield only marginal effects on the computed dissociation energies of Ag(I) complexes as compared to MP2 calculations with the same basis set. This indicates the relatively small significance of dynamic electron correlation effects, which would have better been accounted for by MP4 than by MP2.³⁸

The contribution of relativistic effects to the energy and geometry of the Ag(I)–C₂H₄ complex is evaluated using the RESC approximation.¹⁹ The calculated RESC correction to the dissociation energy is $-0.4 \text{ kcal}\cdot\text{mol}^{-1}$ at both RHF/SBK(d) and MP2/SBK(d) levels, or ca. 1% of the calculated Ag(I)–C₂H₄ interaction energy (Table 2). RESC calculations of silver(I) complexes with neutral nuclei, AgX, also predict minor changes of their RHF and MP2 dissociation energies. In addition, RESC relativistic corrections to the bond dissociation energy of even AgH, which is most prone to relativistic effect due to the short Ag–H bond, amount to only $4 \text{ kcal}\cdot\text{mol}^{-1}$.¹⁹ Therefore, it seems to be the case that the earlier estimate of the relativistic component of ca. $10 \text{ kcal}\cdot\text{mol}^{-1}$ using EDA¹⁵ is exaggerated, and should most probably be attributed to the known shortcomings of the energy decomposition scheme of Morokuma.^{10c}

C. Ag(I) Complexes with Multiple Alkene Ligands.

Multiple coordination of unsaturated organic compounds to silver is firmly established experimentally, e.g., via the detection of Ag(CO)_n and Ag⁺(CO)_n complexes in a solid neon matrix,³⁹ CO₂ complexes with silver halides in solid argon matrix,⁴⁰ or foremost solid AgBF₄·(C₂H₄)_n complexes,² with $n = 1-3(4)$. Nevertheless, previous theoretical studies only consider alkene–Ag(I) complexes with a single ligand.^{4,15} Since the long-term aim of this study includes a detailed study of Ag(I) complexes with terpenes that have multiple double bonds, a systematic study of complexes with more than one C=C ligand is demanded. The two major questions in this regard are the following: (a) What is the maximum coordination number of Ag(I) with alkenes: 2 or higher? (b) What is the arrangement of ligands around the silver nucleus? Ag(I) has a $4d^{10}$ -electron shell, which presumes that ligands up to coordination number $n = 4$ should be feasible to satisfy the 18-electron rule. We also were interested in higher coordination numbers. Therefore, complexes of the formula Ag(I)–(C₂H₄)_n with $n = 2-4$ and 6 were studied at the MP2/SBK(d) level, and the results reported in Figures 3–6 and in Table 3.

Our calculations for $n = 2-4$ complement the known T-shaped^{4,15} (with hydrogen out of the T-plane) C_{2v} structure of Ag(I)–C₂H₄ by ‘multiple T’ structures of Ag(I)–(C₂H₄)_n. These model structures display the symmetry predicted by a classic analysis of transition metal–ethene complexes,⁴¹ and are found to be minima on the corresponding potential energy surfaces by vibrational frequency analysis. This confirms that

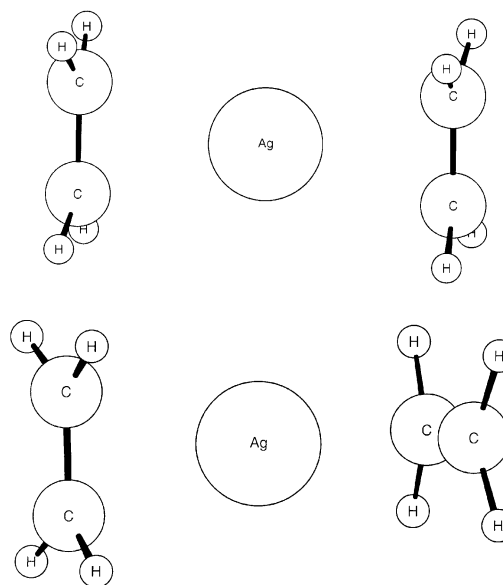


Figure 3. D_{2h} (top) and D_{2d} (bottom) Ag(I)–(C₂H₄)₂ complexes.

TABLE 3: Binding Enthalpies of Silver(I) Complexes with Ethylene Ligands (MP2/SBK(d) Computations)

species	ΔE (kcal·mol ⁻¹)
Ag ⁺ –C ₂ H ₄	–33.7
Ag ⁺ –2C ₂ H ₄ ; planar (D_{2h})	–69.0
Ag ⁺ –2C ₂ H ₄ ; perpendicular (D_{2d})	–68.7
Ag ⁺ –3C ₂ H ₄	–91.8
Ag ⁺ –4C ₂ H ₄	–103.3
Ag ⁺ –6C ₂ H ₄	–112.8

such qualitative symmetry considerations are indeed also valid for Ag(I) complexes.

1. $n = 2$. For Ag(I)–(C₂H₄)₂, two conformations are found, having D_{2h} and D_{2d} symmetry (Figure 3). For both complexes, the addition of the second ethene ligand to Ag(I) is predicted to occur with approximately the same energy gain as the complexation of the first ethene ligand (Table 3).

The complexation of the second ethene ligand is computed to occur with an enthalpy of complexation of $35.3 \text{ kcal}\cdot\text{mol}^{-1}$, i.e., similar to ΔH for the first ($33.7 \text{ kcal}\cdot\text{mol}^{-1}$). This phenomenon has also been observed experimentally: ΔH was found to be 33.7 and $32.4 \text{ kcal}\cdot\text{mol}^{-1}$ by ICR experiments.³⁵ This similarity in binding enthalpies for the first and second ligands has also been found for isoprene (39.2 and $38.5 \text{ kcal}\cdot\text{mol}^{-1}$, respectively),⁴² 2-pentene (37.8 and $39.0 \text{ kcal}\cdot\text{mol}^{-1}$),⁴² and acetone (38.3 and $40.8 \text{ kcal}\cdot\text{mol}^{-1}$).⁴² Therefore, the observation that the first and second dissociation energies are similar for the complexes of organic π -systems with Ag(I) seems to be a general one, and in fact one that seems applicable to a larger series of transition metals. For example, the dissociation energy of Cu(I)–(C₂H₄)₂ is $41.5 \text{ kcal}\cdot\text{mol}^{-1}$ vs $42.0 \text{ kcal}\cdot\text{mol}^{-1}$ for Cu(I)–(C₂H₄),⁴³ while the metal–ethene complexes in the series V, Cr, Mn, Fe all have even slightly higher energies of attachment of the second ligand than of the first one.⁴³ Given the remarkable successes of DFT in transition metal chemistry, it is noteworthy that B3LYP does not yield this result, with either the SBK(d) or the LANL2DZ basis sets: with SBK(d), ΔH was found to be 41.4 and $35.2 \text{ kcal}\cdot\text{mol}^{-1}$ for the first and second ethene ligands, respectively, while with the LANL2DZ basis set these values were -33.5 and $28.3 \text{ kcal}\cdot\text{mol}^{-1}$, respectively.⁴⁴

The predicted strong binding of second ethene ligand to Ag(I) can be readily explained by the HOMO orbital picture,

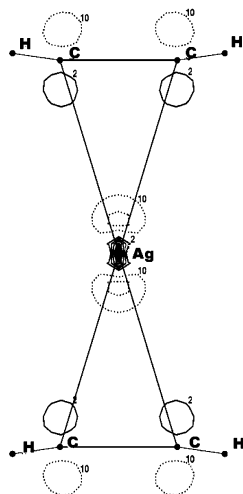


Figure 4. HOMO isodensity map for planar D_{2h} $\text{Ag(I)}-(\text{C}_2\text{H}_4)_2$ [MP2/SBK(d) computation]. The notations 2 and 10 respectively correspond to positive and negative density contours of 0.125 e.

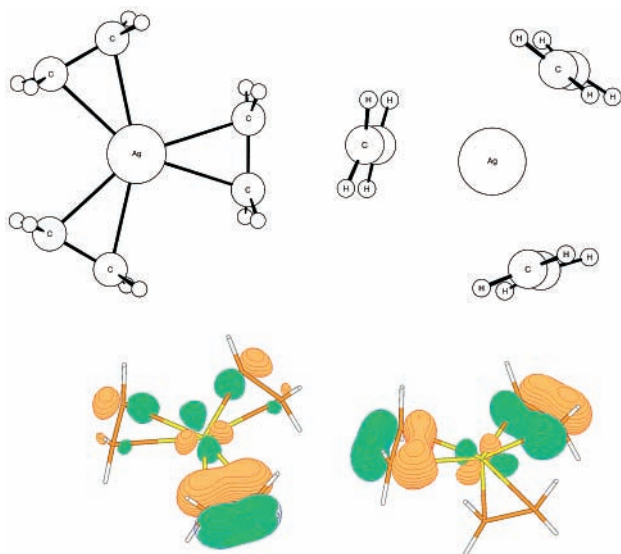


Figure 5. The two D_{3h} , “spoke wheel” (top left) and “barrel” (top right) $\text{Ag(I)}-(\text{C}_2\text{H}_4)_3$ complexes, together with the degenerate set of HOMOs for the spoke wheel complex (bottom).

(Figure 4). A small but clear sandwich-type overlap of the π -orbitals of the two ethene molecules with a d-orbital of Ag(I) in between is observable (vertically oriented in Figure 4, left and right from the Ag nucleus). The increased size of this π -d- π bonding region apparently compensates the induced dipole-induced dipole repulsion between the two ethene ligands.

This also explains the approximately similar stability of the perpendicular structure. In this structure, the extended π -d- π bonding does not exist (the ethene ligands bind to perpendicular d-orbitals of the metal), but the electrostatic repulsion between the two π -systems is also diminished. The overall picture, therefore, is that the loss of covalent stabilization is compensated by the diminished electrostatic destabilization.

2. $n = 3$. No ICR or other experimental data have been reported on Ag(I) complexes with three and more alkene ligands. Our investigations concentrated on two D_{3h} complexes for $n = 3$, namely, a spoke-wheel and a barrel conformation such as depicted in Figure 5. The planar trigonal, “spoke wheel” structure (Figure 5, top left) is a real minimum, as shown by vibrational frequency computations, but the “barrel” conforma-

tion (Figure 5, top right) is not, and has three imaginary frequencies. Computation of the complexation enthalpies shows that the third ethene molecule enters the coordination sphere of Ag(I) with less energy gain than the first two, namely, $22.7 \text{ kcal}\cdot\text{mol}^{-1}$ vs ca. $34\text{--}35 \text{ kcal}\cdot\text{mol}^{-1}$. The reason for the reduced dissociation energy of the third ethene molecule in the planar trigonal minimum of $\text{Ag(I)}-(\text{C}_2\text{H}_4)_3$ can be interpreted as steric, as the minimal distance between carbon atoms of different ethene ligands in this complex is 3.32 \AA , and the minimal C–H distance 2.17 \AA . The orbital representations of the degenerate set of HOMOs (Figure 5, bottom) also point to a diminished orbital overlap, which is in line with the computed lower binding energy. A precise evaluation, i.e., within a few kcal/mol, of the complexation energies for the third ethene ligand will therefore await the applicability of higher level computations, since the Ag-C distance, and therefore the steric effects in the trigonal planar cluster, will be critically dependent on the theoretical level. Since our benchmark data (both *vide infra* and *vide supra*) include only complexes with one or two ligands, a proper check also awaits additional experiments. Nevertheless, since the difference between the complexation enthalpies of the second and third ethene is larger than $10 \text{ kcal}\cdot\text{mol}^{-1}$, and in line with qualitative considerations, it seems prudent to state that the third ligand binds significantly weaker to the silver cation than the first and second ethene ligands. On the other hand, the discovery of a rather stable minimum with $n = 3$ points to the relevance of triply bound Ag(I) -alkene complexes, as may occur in the Ag complexation of certain flexible terpenes.³

3. $n = 4$. With four molecules of ethene, two complexes with D_{4h} skeletal symmetry were studied, namely, the “square planar” and “barrel” conformations, in addition to a tetrahedron-like arrangement (Figure 6). The first configuration has been dismissed in early analyses as highly unfavorable for steric reasons,⁴¹ and the lack of any practical relevance was confirmed by the computation of both a relatively high energy ($29 \text{ kcal}\cdot\text{mol}^{-1}$ with respect to the tetrahedral structure) and the presence of seven imaginary vibrational frequencies. The “barrel” D_{4h} configuration is considerably lower in energy than the “square planar” complex ($14 \text{ kcal}\cdot\text{mol}^{-1}$ with respect to the tetrahedral structure), but still has three imaginary vibrational frequencies. The most stable configuration of $\text{Ag(I)}-(\text{C}_2\text{H}_4)_4$ is an approximately tetrahedral structure. For this complex, the dissociation energy of the fourth C_2H_4 ligand is $11.5 \text{ kcal}\cdot\text{mol}^{-1}$ (with reference to the most stable, planar trigonal $\text{Ag(I)}-(\text{C}_2\text{H}_4)_3$ complex; MP2/SBK(d) computations), i.e., significantly lower again than the third ethene ligand, but still clearly bound.

4. $n = 6$. The largest complex under study comprises the silver cation with six ethene ligands in an octahedral-like coordination. The structure (Figure 7) was obtained from the addition of an ethene molecule to each of the axial positions to the ‘barrel’-like structure for $n = 4$, and has C_2 symmetry. As can be seen in Table 3, the addition of the fifth and sixth ethene ligand is accompanied by an increasingly smaller enthalpic gain: the average value for $\Delta H = 4.8 \text{ kcal}\cdot\text{mol}^{-1}$, down from $11.5 \text{ kcal}\cdot\text{mol}^{-1}$ for the fourth ligand. Given the entropic loss that will be accompanied by complexation of ethene ligands, it is questionable whether the $n = 6$ species, although a minimum on the potential energy surface, will be an observable species.

D. Ag(I) -Alkene Complexes of Methyl-Substituted Alkenes. To complete this study of the factors that influence the complexation of natural compounds such as terpenes, the influence of alkyl substitution on the alkenes was investigated. To this aim, the structures of all complexes of the form

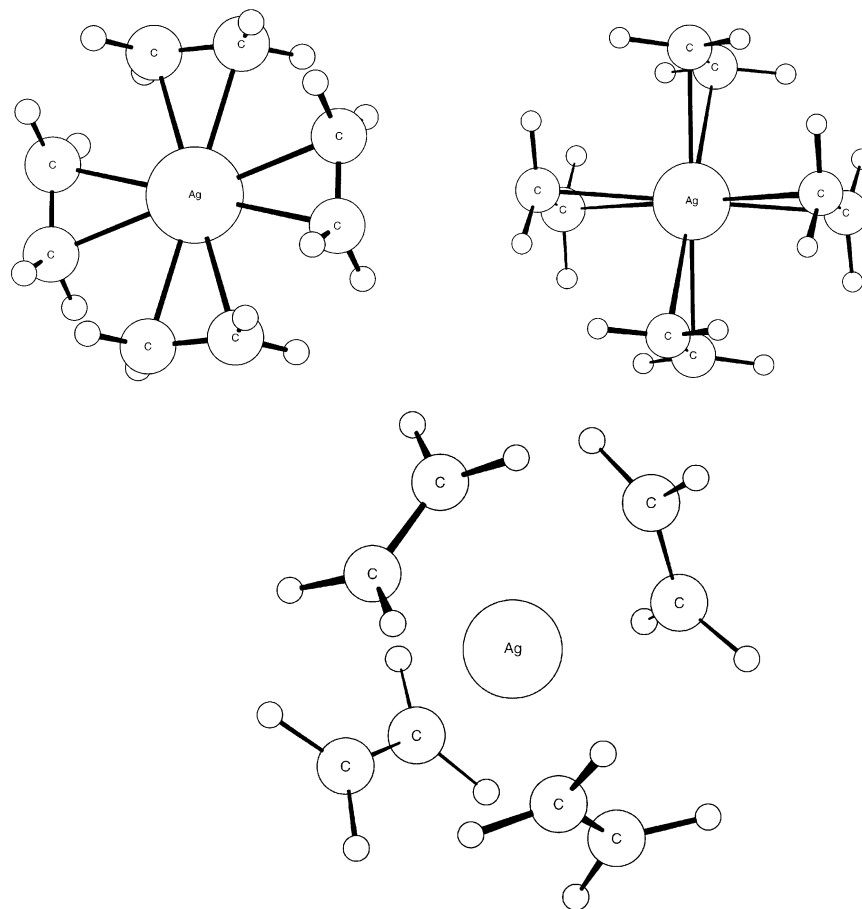


Figure 6. The “square planar” (top left), “barrel” (top right), and stable “tetrahedral” (bottom) configurations of the $\text{Ag}^+(\text{C}_2\text{H}_4)_4$ complex [MP2/SBK(d) computations].

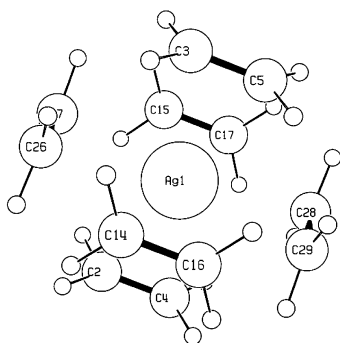


Figure 7. The octahedral-like $\text{Ag}^+(\text{C}_2\text{H}_4)_6$ complex [MP2/SBK(d) computation].

$\text{Ag}(\text{I})-\text{C}_2\text{H}_4-x(\text{CH}_3)_x$ were optimized at the MP2/SBK(d) level, and their complexation enthalpies computed (see Table 4). These complexation enthalpies are compared to experimental data obtained both by ICR experiments⁴² and by the corresponding capacity factors K' that have been measured for these alkenes by argentation chromatography by Van Beek and Subrtova.³

The data in Table 4 unequivocally predict the complexation of alkenes to silver cation to strengthen with increased methyl substitution. The measured ICR value for isoprene (2-methyl-2-butene) is $39.2 \text{ kcal}\cdot\text{mol}^{-1}$,⁴² which agrees with the computed value within the limits of the ICR experiment, again supporting the choice of computational method. The stronger complexation can be linked to the energy of the highest occupied molecular orbital (HOMO) and—to a lesser extent, given the nature of the silver–alkene interactions—to the lowest unoccupied

TABLE 4: Calculated Binding Enthalpies ΔH and Experimental Capacity Factors K' of Methyl-Substituted Ag(I) Complexes

alkene	ΔH_{calc} ($\text{kcal}\cdot\text{mol}^{-1}$)	K_{calc}^a	K'
ethene	−33.7	1.7×10^{25}	1.32
propene	−36.6	2.5×10^{27}	0.98
(<i>Z</i>)-2-butene	−38.0	2.8×10^{28}	0.49
(<i>E</i>)-2-butene	−38.3	4.7×10^{28}	0.27
2-methyl-2-butene	−41.3	8.3×10^{30}	0.16
2,3-dimethyl-2-butene	−43.5	3.7×10^{32}	0.04

^a K_{calc} was for reasons of simplicity computed at $T = 293 \text{ K}$ under the assumption that $\Delta S = 0$, to be able to compare trends in the computed and experimental K -values (which hinge on the assumption that for the various alkenes $\Delta\Delta S = 0$).

molecular orbital (LUMO) upon methyl substitution. An increase in the HOMO energy will improve the $\pi \rightarrow s^*$ electron donation, and strengthen the silver(I)–alkene bond; a decrease in the LUMO energy will improve the $d \rightarrow \pi^*$ electron back-donation. Since methyl substitution generally increases the HOMO energy significantly, but only affects the LUMO energies to a much smaller degree, the overall general effect is expected to be an increase of the strength of the silver–alkene bond on methyl substitution.

These predictions can be illustrated for the ethene versus isoprene case, which is chosen to allow for direct comparison to experiment. The HOMO energy increases by almost 2 eV from −15.95 eV in Ag(I)–ethene to −14.06 eV in Ag(I)–isoprene; the corresponding LUMO energies also increase, but only by 0.25 eV, from −3.80 to −3.55 eV. This implies an

increased electronic component in the complexation (strongly increased $\pi \rightarrow s^*$ electron donation, and only a small further reduction of the already weak $d \rightarrow \pi^*$ electron back-donation), and therefore a strengthening of the silver–alkene bonding. Apparently this is not offset by any steric effects. The large distances between any of the methyl carbon and hydrogen atoms and the silver cation ($>3.1 \text{ \AA}$) suggest that in these complexes steric effects that may arise on complex formation are expected to be rather small, and this is in line with the given model.

Since the computed data for both ethene and isoprene (Table 4, entries 1 and 5) agree within experimental error with the gas-phase experiment, this gives a solid basis for the computed trend in complexation enthalpies. Therefore, the strong differences in trends between the gas-phase complexation enthalpies and the experimental chromatography data point to decisive effects of the medium. The changes in chromatographic retention between methyl-substituted alkenes may therefore be related to trends in solvation properties of these alkenes, or to specific interactions these materials may have with the solid support. In this light, it seems desirable to reinvestigate several of the aspects of argentation chromatography, to better understand the factors that form the basis of this successful experimental technique. Since the MP2 computations seem to be somewhat more accurate than the corresponding B3LYP ones, the recent advance of local MP2 techniques is of specific interest, as this will allow for the investigation of significantly larger complexes and/or larger basis sets. Such investigations (both experimental and theoretical) are currently underway in our laboratories.

Conclusions

A systematic comparison of three computational methodologies, B3LYP, RHF, and MP2, in combination with several moderate size basis sets shows the MP2/SBK(d) approach to be sufficiently accurate and computationally efficient for studies of silver(I)–alkene complexes. We show that cationic complexes of Ag(I) may accommodate up to four alkene ligands. Our MP2 calculations reproduce well the known experimental gas-phase trends in complexation energies of Ag(I) with multiple alkene ligands, as well as in Ag(I) complexes with methyl-substituted ethenes. The trend in the latter (stronger complexation with increased methyl substitution) contrasts with the trend found in argentation chromatography, which thus seems dominated by medium effects.

Acknowledgment. We thank Dr. Teris van Beek (Wageningen University), Dr. Boryana Nikolova Damyanova (Bulgarian Academy of Sciences), and Dr. Alexandr Voityuk (TU Munich) for helpful discussions. In addition, we thank Dr. Albert van der Padt (Wageningen University) for a fruitful collaboration in this area. Thanks are also due to Arnold Bosch for computational assistance, and to the referees of a previous version of this paper for many stimulating suggestions.

References and Notes

- (1) (a) Ma, J. C.; Dougherty, D. A. *Chem. Rev.* **1997**, *97*, 1303. (b) Gokel, G. W.; De Wall, S. L.; Meadows, E. S. *Eur. J. Org. Chem.* **2000**, 2967–2978.
- (2) Powell, P. *Principles of Organometallic Chemistry*, 2nd ed.; Chapman & Hall: New York, 1988.
- (3) van Beek, T. A.; Subrtova, D. *Phytochem. Anal.* **1995**, *6*, 1–19.
- (4) Frenking, G.; Froehlich, N. *Chem. Rev.* **2000**, *100*, 717–774.
- (5) (a) Dewar, M. J. S. *Bull. Soc. Chim. Fr.* **1951**, *18*, C79. (b) Chatt, J.; Duncanson, L. A. *J. Chem. Soc.* **1953**, 2929.
- (6) Cioslowski, J. In *Encyclopedia of Computational Chemistry*; Schleyer, P. v. R., Allinger, N. L., Kollman, P. A., Clark, T., Schaefer, H. F. S., Gasteiger, J., Schreiner, P. R., Eds.; Wiley-VCH: Chichester, 1998; Vol. 2, p 892.
- (7) Reed, A. E.; Curtiss, L. A.; Weinhold, F. *Chem. Rev.* **1988**, *88*, 899. See also Weinhold, F., ref 6, Vol. 3, p 1792.
- (8) Dapprich, S.; Frenking, G. *J. Phys. Chem.* **1995**, *99*, 9352.
- (9) (a) Bader, R. F. W. *Atoms in Molecules. A Quantum Theory*; Oxford University Press: Oxford, 1990. (b) Bader, R. F. W., in ref 6, Vol. 1, p 64.
- (10) (a) Morokuma, K. *J. Chem. Phys.* **1971**, *55*, 1236–1244. (b) Kitaura, K.; Morokuma, K. *Int. J. Quantum Chem.* **1976**, *10*, 325. (c) See also: Gordon, M. S.; Jensen, J. H. in ref. 6, vol. 5, p 3198, in particular pp 3204–3205.
- (11) Ziegler, T.; Rauk, A. *Theor. Chim. Acta* **1977**, *46*, 1.
- (12) (a) Bagus, P. S.; Hermann, K.; Bauschlicher, C. W. *J. Chem. Phys.* **1984**, *80*, 4378. (b) Stevens, W. J.; Fink, W. H. *Chem. Phys. Lett.* **1987**, *139*, 15–22.
- (13) (a) Sodupe, M.; Bauschlicher, C. W., Jr. *J. Phys. Chem.* **1991**, *95*, 8640. (b) Miralles-Sabater, J.; Merchán, M.; Nebot-Gil, I.; Viruela-Martín, P. M. *J. Phys. Chem.* **1988**, *92*, 4853. (c) See also: Sodupe, M.; Bauschlicher, C. W., Jr.; Langhoff, S. R.; Partridge, H. *J. Phys. Chem.* **1992**, *96*, 2118.
- (14) Ziegler, T.; Rauk, A. *Inorg. Chem.* **1979**, *18*, 1558.
- (15) Hertwig, R. H.; Koch, W.; Schröder, D.; Schwartz, H.; Hrusák, J.; Schwerdtfeger, P. *J. Phys. Chem.* **1996**, *100*, 12253–12260.
- (16) Ma, N. L. *Chem. Phys. Lett.* **1998**, *297*, 230–238.
- (17) Pyykkö, P. *Chem. Rev.* **1988**, *88*, 563.
- (18) Pisani, L.; André, J.-M.; André, M.-C.; Clementi, E. *J. Chem. Educ.* **1993**, *70*, 894.
- (19) Nakajima, T.; Hirao, K. *Chem. Phys. Lett.* **1999**, *302*, 383–391.
- (20) (a) Becke, A. D. *J. Chem. Phys.* **1993**, *98*, 5648. (b) Lee, C.; Yang, W.; Parr, R. G. *Phys. Rev.* **1988**, *B37*, 785. (c) Stephens, P.; Devlin, F. J.; Chabalowski, C. F.; Frisch, M. J. *J. Phys. Chem.* **1994**, *98*, 11623.
- (21) Hay, P. J.; Wadt, W. R. *J. Chem. Phys.* **1988**, *82*, 270–283.
- (22) (a) Stevens, W. J.; Basch, H.; Krauss, M. *J. Chem. Phys.* **1984**, *81*, 6026–6033. (b) Stevens, W. J.; Basch, H.; Krauss, M. *Can. J. Chem.* **1992**, *70*, 612–630. (c) Cundari, T. R.; Stevens, W. J. *J. Chem. Phys.* **1993**, *98*, 5555–5565.
- (23) *Gaussian 98*, Revision A.7: Frisch, M. J.; Trucks, G. W.; Schlegel, H. B.; Scuseria, G. E.; Robb, M. A.; Cheeseman, J. R.; Zakrzewski, V. G.; Montgomery, J. A., Jr.; Stratmann, R. E.; Burant, J. C.; Dapprich, S.; Millam, J. M.; Daniels, A. D.; Kudin, K. N.; Strain, M. C.; Farkas, O.; Tomasi, J.; Barone, V.; Cossi, M.; Cammi, R.; Mennucci, B.; Pomelli, C.; Adamo, C.; Clifford, S.; Ochterski, J.; Petersson, G. A.; Ayala, P. Y.; Cui, Q.; Morokuma, K.; Malick, D. K.; Rabuck, A. D.; Raghavachari, K.; Foresman, J. B.; Cioslowski, J.; Ortiz, J. V.; Stefanov, B. B.; Liu, G.; Liashenko, A.; Piskorz, P.; Komaromi, I.; Gomperts, R.; Martin, R. L.; Fox, D. J.; Keith, T.; Al-Laham, M. A.; Peng, C. Y.; Nanayakkara, A.; Gonzalez, C.; Challacombe, M.; Gill, P. M. W.; Johnson, B.; Chen, W.; Wong, M. W.; Andres, J. L.; Gonzalez, C.; Head-Gordon, M.; Replogle, E. S.; and Pople, J. A. Gaussian Inc., Pittsburgh, PA, 1998.
- (24) Hay, P. J.; Wadt, W. R. *J. Chem. Phys.* **1988**, *82*, 284, 299, plus Los Alamos ECP (ref 21).
- (25) (a) Fuentealba, P.; Preuss, H.; Stoll, H.; Szentpaly, L. v. *Chem. Phys. Lett.* **1989**, *89*, 418. (b) Wedig, U.; Dolg, M.; Stoll, H.; Preuss, H. In *Quantum Chemistry: The Challenge of Transition Metals and Coordination Chemistry*; Veillard, A., Ed.; Reidel: Dordrecht, The Netherlands, 1986, p 79.
- (26) Möller, C.; Plesset, M. S. *Phys. Rev.* **1934**, *46*, 618.
- (27) GAMESS US: Schmidt, M. W.; Baldridge, K. K.; Boatz, J. A.; Elbert, S. T.; Gordon, M. S.; Jensen, J. H.; Koseki, S.; Matsunaga, N.; Nguyen, K. A.; Su, S. J.; Windus, T. L.; Dupuis, M.; Montgomery, J. A. *J. Comput. Chem.* **1993**, *14*, 1347–1363.
- (28) (a) Kestner, N. R.; Combariza, J. E. In *Reviews in Computational Chemistry*; Lipkowitz, K. B., Boyd, D. B., Eds.; J. Wiley & Sons: New York, 1999; Vol. 13, pp 99–131. (b) Jensen, F. *Introduction to Computational Chemistry*; J. Wiley & Sons: New York, 1999, pp 172–173.
- (29) Schaftenaar, G. <http://www.cmbi.kun.nl/~schaft/molden/molden.html>.
- (30) <http://www.camsoft.com>.
- (31) Koch, W.; Holthausen, M. C. A *Chemist's Guide to Density Functional Theory*; Wiley-VCH: Weinheim, 2000.
- (32) Böhme, M.; Wagener, T.; Frenking, G. *J. Organomet. Chem.* **1996**, *520*, 31.
- (33) Moore, C. E. *Atomic Energy Levels*; National Bureau of Standards; U. S. Government Printing Office: Washington, DC, 1949.
- (34) (a) Douglas, M.; Kroll, N. M. *Ann. Phys. (N.Y.)* **1974**, *82*, 89. (b) Hess, B. A. *Phys. Rev.* **1985**, *A32*, 756. (c) Hess, B. A. *Phys. Rev.* **1986**, *A33*, 3742.
- (35) Guo, B. C.; Castleman, A. W., Jr. *Chem. Phys. Lett.* **1991**, *181*, 16–20.
- (36) Huang, H. Y.; Padin, J.; Yang, R. *J. Phys. Chem. B* **1999**, *103*, 3206–3212.

(37) (a) Frenking, G.; Antes, I.; Böhme, M.; Dapprich, S.; Ehlers, E. W.; Jonas, V.; Neuhaus, A.; Otto, M.; Stegmann, R.; Veldkamp, A.; Vyboishchikov, S. F. In *Reviews in Computational Chemistry*; Lipkowitz, K. B., Boyd, D. B., Eds.; J. Wiley & Sons: New York, 1996; Vol. 8, pp 63–144. (b) Helgaker, T.; Taylor, P. R. In *Modern Electronic Structure Theory, Part II*; Yarkony, D. R., Ed.; World Scientific: Singapore, 1995.

(38) Martin, J. M. L. in ref 6, vol. 1, 115–128.

(39) Liang, B.; Andrews, L. *J. Phys. Chem. A* **2000**, *104*, 9156–9164.

(40) Zhou, M.; Zhang, L.; Chen, M.; Qike, Z.; Qizong, Q. *J. Phys. Chem. A* **2000**, *104*, 10159–10164.

(41) Roesch, N.; Hoffmann, R. *Inorg. Chem.* **1974**, *13*, 2656–2666.

(42) Ho, Y.-P.; Yang, Y.-C.; Klippenstein, S. J.; Dunbar, R. C. *J. Phys. Chem.* **1997**, *101*, 3338–3347.

(43) Sievers, M. R.; Jarvis, L. M.; Armentrout, P. B. *J. Am. Chem. Soc.* **1998**, *120*, 1891–1899.

(44) LANL2DZ for Ag, and 6-311G(d,p) for C and H.